JOURNAL OF MAGNETIC RESONANCE **133,** 70–78 (1998)
ARTICLE NO. MN981433

Spectral Editing Technique for the *in Vitro* and *in Vivo* Detection of Taurine

D. L. Hardy and T. J. Norwood

Department of Chemistry, University of Leicester, University Road, Leicester, LE1 7RH, United Kingdom

Received March 7, 1997; revised January 28, 1998

***In vivo* ^{1}H NMR spectroscopy has proven to be a useful noninvasive tool for the investigation of numerous metabolic and physiological states. Taurine is potentially a useful indicator in neonate development and is involved in a number of physiological processes. However, it could not previously be observed in the *in vivo* ^{1}H spectrum because of overlap with adjacent resonances. We have developed a spectral editing technique based upon double quantum filtration which allows the taurine resonances to be resolved from adjacent peaks. The experiment is demonstrated both on perchloric acid rodent brain extract and on rodent brain homogenate.** © 1998 Academic Press

INTRODUCTION

In vivo ^{1}H NMR spectroscopy has proven to be a useful tool in the investigation of numerous metabolic states in developing rodents and humans. Unfortunately, spectral overlap is common as a consequence of the low magnetic field strengths normally available and the broad lines of most resonances. Consequently, relatively few metabolites can be discerned unambiguously.

Although thought somewhat inert, taurine has steadily shown its importance in many biological areas (*1, 2*). These range from a possible neurotransmitter role (*3*) in the central nervous system and retina to involvement in a number of physiological (*4*) actions such as osmoregulation (*5–7*), calcium modulation, and antioxidation (for which taurine is the product). Taurine is found in high concentration at birth, decreasing rapidly with age (*8*). The reason for such a high concentration is still unclear, but is thought to be linked to the cellular functions which are important in neonate development. Some *in vivo* studies have been carried out on the developing brain (*9*), with most work being restricted to *in vitro* experiments (*10, 11*). Previous attempts to observe taurine *in vivo* have failed to totally resolve it from the surrounding overlapping metabolites (*12*). Although taurine has been measured in excised rat brain at 360 MHz using a double irradiation technique (*13*), this method requires the selective irradiation of just one of its multiplets and consequently is not applicable at low magnetic field strengths or *in vivo.* A noninvasive technique which could monitor these changes would provide a useful insight into the metabolic changes associated with the developing brain.

In vivo NMR spectroscopy is limited by a number of factors which govern the spectral resolution and the structure of pulse sequences which can be used and therefore its usefulness. The contributing factors are short transverse relaxation times, which result in rapid loss of signal in multiple pulse experiments as well as broadening of the spectral lines; magnetic field inhomogeneity, which also leads to a broadening of the spectral lines; and the use of low static magnetic field strengths, which results in increased spectral overlap. In a typical *in vivo* spectrum few metabolites can be measured unequivocally without resort to spectral editing.

NMR editing techniques designed for use *in vivo* must be able to cope with poor spectral resolution due to low static magnetic field strengths (B_0), must be relatively short to minimize any signal loss due to transverse relaxation, and must be robust enough to cope with B_0 and applied magnetic field (B_1) variations across the sample, particularly if they are to be implemented with a surface coil. Because of these criteria, the most useful tools for *in vivo* spectroscopy have been found to be semiselective pulses (*14, 15*) giving low-selectivity chemical shift selection (*16–18*) and multiple quantum filters (MQFs) for editing according to the number of coupled spins (*19–26*).

In this paper we describe a new editing technique that enables taurine to be detected *in vivo* and *in vitro.* Development of the pulse sequence is shown on a rat brain perchloric acid (PCA) extract and on rat brain homogenate.

THEORY

Before deciding upon the appropriate technique to edit for a particular metabolite it is first necessary to consider the spectroscopic properties of both the selected metabolite and those of any other metabolite that overlap with it in the NMR spectrum. Taurine is an AA′XX′ spin system, but for simplicity and because of the low field strengths typically used *in vivo,* it can be considered to have an A_2X_2 spin system for the purpose of analysis. The ^{1}H spectrum of taurine contains two ‘‘triplets’’ which appear at 3.27 ppm (NCH_2) and 3.43 ppm

1090-7807/98 $25.00
Copyright © 1998 by Academic Press
All rights of reproduction in any form reserved.

(SCH_2) in the spectra of both human and rodent brain extract at physiological pH (Fig. 1a). The 3.43-ppm taurine multiplet is relatively clear from overlapping metabolites and is clearly seen in the *in vitro* ^{1}H spectrum, with the 3.27-ppm taurine multiplet being obscured by the [5]CH myo-inositol multiplet (3.28 ppm) and, depending on the ischemic state, the ethanolamine NCH_2 multiplet (3.15 ppm). However, *in vivo* the 3.43-ppm taurine multiplet is engulfed by the [1,3]CH myo-inositol (3.54 ppm) and the N–CH_2 choline (3.54 ppm) multiplets, along with the glycine singlet (3.56 ppm). In addition, *in vivo* the 3.27-ppm taurine multiplet overlaps with the singlets of choline (3.20 ppm), phosphocholine (3.21 ppm), and glycerophosphocholine (3.22 ppm). It can be seen that a large number of the overlapping metabolite resonances are singlets. A method which removes these singlets would present the best form of initial editing.

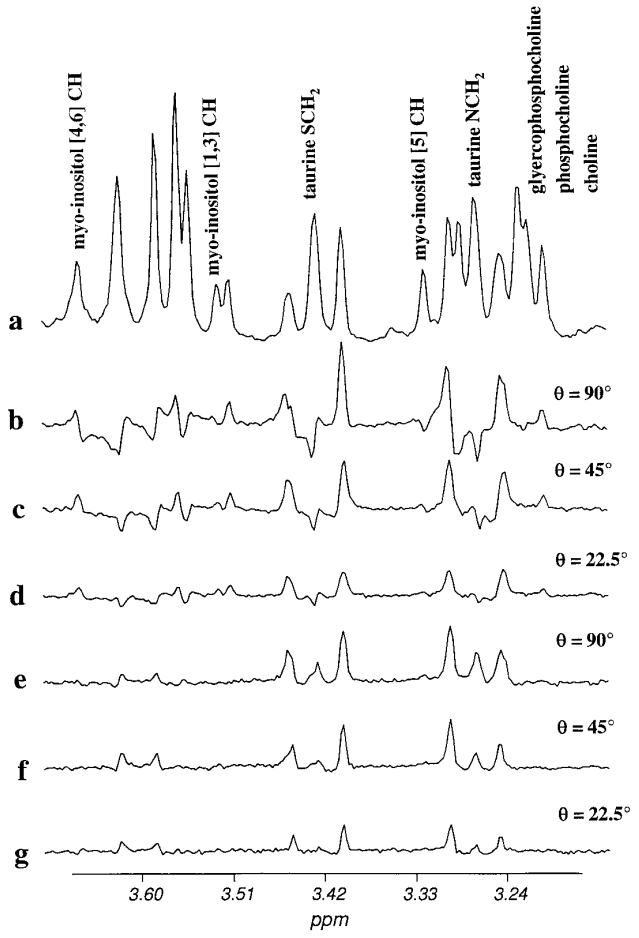

FIG. 1. Proton spectra at 250 MHz of a perchloric acid extract from a rat brain. (a) Conventional 1D sequence with taurine and other important multiplets labeled. (b–d) DQF spectra obtained using the pulse sequence given in Fig. 2a using a τ value of 50 ms, a τ' value of 40 ms, and read pulse angles θ of (b) 90°, (c) 45°, and (d) 22.5°. (e–g) Spectra obtained using the pulse sequence given in Fig. 2b using 20-ms Gaussian pulses placed in between the two taurine multiplets (3.35 ppm) with $\tau = 44$ ms, $\tau' = 40$ ms, with read pulse angles θ of (e) 90°, (f) 45°, and (g) 22.5°. All spectra are displayed to the same vertical scale.

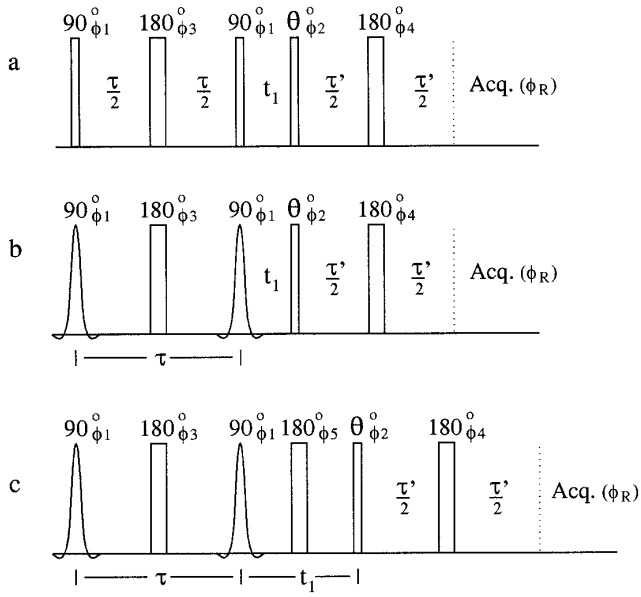

FIG. 2. Pulse sequences for double-quantum filtration. (a) Pulse sequence incorporating a refocusing period to produce in-phase spectra and a variable read angle pulse. (b) Pulse sequence as in (a), but incorporating soft pulses for additional selectivity. (c) Pulse sequence as in (b), but with spin echo during the evolution period (t_1) to refocus any chemical shift evolution. Phase cycling where applicable: $\phi_1 = (x, y, -x, -y)$; $\phi_2 = (x, x, x, x, -x, -x, -x, -x)$; $\phi_3 = 4(x, y, -x, -y)$, $4(-x, -y, x, y)$; $\phi_4 = 8(x)$, $8(-x)$; $\phi_5 = 32(y)$, $32(-y)$; and $\phi_R = (x, -x, x, -x, -x, x, -x, x)$.

MQFs have been proven to be one of the most useful and simplest editing techniques for *in vivo* ^{1}H spectroscopy (*27–35*). By using an MQF of a particular order it is possible to filter out spin systems that cannot attain that order of coherence. That is, a double quantum filter (DQF) will filter out any singlets in the spectrum. MQFs have a number of advantages over other more sophisticated editing techniques when used *in vivo.* MQFs are simple to construct and implement since they contain few pulses, are relatively efficient, and are also unaffected by magnetic-field inhomogeneities.

The pulse sequence that forms the basis of double quantum filters used *in vivo* can be seen in Fig. 2a. Considering taurine as an A_2X_2 spin system, the effect of the preparation period of this experiment can be calculated using the product operator formalism (*36*):

$$
\begin{aligned}
2(I_{Az} + I_{Xz}) \xrightarrow{90^\circ_x\, \tau/2\ 180^\circ_x\, \tau/2} & \\
&+ 2I_{Ax}I_{Xz}4\cos(\pi J_{AX}\tau)\sin(\pi J_{AX}\tau) \\
&+ 2I_{Az}I_{Xx}4\cos(\pi J_{AX}\tau)\sin(\pi J_{AX}\tau) \\
&+ 4I_{Ay}I_{Xz}I_{Xz}2\sin^2(\pi J_{AX}\tau) \\
&+ 4I_{Xy}I_{Az}I_{Az}2\sin^2(\pi J_{AX}\tau)
\end{aligned}
$$

$$\xrightarrow{90^\circ_x} -2I_{Ax}I_{Xy}4\cos(\pi J_{AX}\tau)\sin(\pi J_{AX}\tau)$$
$$-2I_{Ay}I_{Xx}4\cos(\pi J_{AX}\tau)\sin(\pi J_{AX}\tau)$$
$$-4I_{Az}I_{Xy}I_{Xy}2\sin^2(\pi J_{AX}\tau)$$
$$-4I_{Xz}I_{Ay}I_{Ay}2\sin^2(\pi J_{AX}\tau), \quad [1]$$

where only terms that will result in DQC are given. The terms on the right side of Eq. [1] correspond to linear combinations of two spin coherences. Pure DQC is given by

$$(\mathrm{DQC})_Y = \tfrac{1}{2}(2I_{Ax}I_{Xy} + 2I_{Ay}I_{Xx}) \quad [2]$$

and

$$(\mathrm{DQC})_x = \tfrac{1}{2}(2I_{Ax}I_{Xx} - 2I_{Ay}I_{Xy}). \quad [3]$$

The DQC created after the preparation consists of three components. Using these equations it can be seen that the first two terms on the right of Eq. [1] consist of pure in-phase DQC between spin A and X given by $-(1/2)(2I_{Ax}I_{Xy} + 2I_{Ay}I_{Xx})8\cos(\pi J_{AX}\tau)\sin(\pi J_{AX}\tau)$. The third and fourth terms correspond to a mixture of antiphase two-spin coherences. Pure DQC arising from the third term is given by $-(1/2)(2I_{Xy}I_{Xy} - 2I_{Xx}I_{Xx})2I_{Az}2\sin^2(\pi J_{AX}\tau)$ and from the fourth term by $-(1/2)(2I_{Ay}I_{Ay} - 2I_{Ax}I_{Ax})2I_{Xz}2\sin^2(\pi J_{AX}\tau)$. The DQC is then turned back into antiphase magnetization by the subsequent 90° pulse:

$$-(1/2)(2I_{Ax}I_{Xy} + 2I_{Ay}I_{Xx})8\cos(\pi J_{AX}\tau)\sin(\pi J_{AX}\tau)$$
$$-(1/2)(2I_{Xy}I_{Xy} - 2I_{Xx}I_{Xx})2I_{Az}2\sin^2(\pi J_{AX}\tau)$$
$$-(1/2)(2I_{Ay}I_{Ay} - 2I_{Ax}I_{Ax})2I_{Xz}2\sin^2(\pi J_{AX}\tau)$$
$$\xrightarrow{90^\circ_x} -(2I_{Ax}I_{Xz} + 2I_{Az}I_{Xx})4\cos(\pi J_{AX}\tau)\sin(\pi J_{AX}\tau)$$
$$-4I_{Xz}I_{Xz}I_{Ay}\sin^2(\pi J_{AX}\tau)$$
$$-4I_{Az}I_{Az}I_{Xy}\sin^2(\pi J_{AX}\tau), \quad [4]$$

where only terms resulting in observable magnetization are given.

A spin echo is usually appended to the end of the pulse sequence, Fig. 2a, to give a predominantly in-phase spectrum (*21*). This aids interpretation and prevents the mutual cancellation of broad transitions that can result in signal loss *in vivo* when antiphase magnetization is detected.

Although a DQF is primarily used to remove singlets from a spectrum, if two overlapping multiplets have different excitation functions, that is, if the DQC arising from one multiplet is at a maximum value while the other is close to its minimum, it may be possible to remove one or the other. Figure 1a shows that the taurine 3.27-ppm multiplet overlaps with the [5]CH of myo-inositol and so its NMR spectroscopic properties must also be considered if it is to be removed.

Myo-inositol is an AMM′NN′X spin system. The effect of the DQF on the myo-inositol [5]CH proton (A) can be calculated using the product operator formalism. Only the A, M, and M′ spin magnetization ultimately affects the intensity of the filtered A spin multiplets.

$$I_{Az} + 2I_{Mz} \xrightarrow{90^\circ_x\ \tau/2\ 180^\circ_x\ \tau/2}$$
$$+2I_{Ax}I_{Mz}2\cos(\pi J_{AM}\tau)\sin(\pi J_{AM}\tau)$$
$$+2I_{Mx}I_{Az}2\sin(\pi J_{AM}\tau)\cos(\pi J_{MN}\tau)$$
$$+4I_{Ay}I_{Mz}I_{Mz}\sin^2(\pi J_{AM}\tau)$$
$$\xrightarrow{90^\circ_x} -(1/2)(2I_{Ax}I_{My} + 2I_{Ay}I_{Mx})2\sin(\pi J_{AM}\tau)$$
$$\times\ \{\cos(\pi J_{AM}\tau) + \cos(\pi J_{MN}\tau)\}$$
$$-(1/2)(2I_{My}I_{My} - 2I_{Mx}I_{Mx})I_{Az}\sin^2(\pi J_{AM}\tau), \quad [5]$$

where only DQCs are given on the right of the equation.

The DQC is then turned back into antiphase magnetization by the subsequent 90° pulse:

$$\xrightarrow{90^\circ_x} -(2I_{Ax}I_{Mz} + 2I_{Az}I_{Mx})\sin(\pi J_{AM}\tau)$$
$$\times\{\cos(\pi J_{AM}\tau) + \cos(\pi J_{MN}\tau)\}$$
$$-(2I_{Mz}I_{Mz} - 2I_{Mx}I_{Mx})I_{Az}(1/2)\sin^2(\pi J_{AM}\tau). \quad [6]$$

The expressions for the intensities of taurine (Eq. [4]) and the myo-inositol [5]CH (Eq. [6]) are superficially similar, with DQC being created by two mechanisms in each case. Singly antiphase single-quantum coherence (SQC) present at the end of the preparation period will be converted into in-phase DQC, which will in turn be converted back into singly antiphase SQC (mechanism m-1). Similarly, doubly antiphase SQC is filtered through as antiphase DQC (mechanism m-2). Since the coupling constant of the myo-inositol [5]CH to [4,6]CH proton is 9.0 Hz and that of the [4,6]CH to [1,3]CH proton is 9.8 Hz, while that of taurine is 6.4 Hz, it would be expected that their maximum and minimum intensities will occur at different values of τ. From the equations it can be clearly seen that magnetization arising from both mechanisms will pass through zero at a time of $1/J$, with a local minimum at $1/2J$. This minimum arises because although the intensity of signal arising from mechanism m-1 is zero, that arising from the m-2 mechanism is close to its maximum.

Given the values of their scalar couplings, calculations suggest that the intensity of the [5]CH proton of myo-inositol will

pass through zero at $1/J$, whereas that of taurine is close to its maximum at $3/4J$. This time could be used to edit out the [5]CH proton of myo-inositol from the spectrum. However it is likely to be >200 ms and so be too long for use *in vivo,* since the short T_2's usually encountered will result in little or no signal being observed. Alternatively, as the taurine signal reaches its first maximum at $1/4J$ the myo-inositol [5]CH signal will be near its first minimum value of $1/2J$. Since the signal amplitude of the [5]CH of myo-inositol at $1/2J$ depends largely on the doubly antiphase SQC (mechanism m-2), it is possible to suppress this relative to the taurine signal, which arises predominantly from singly antiphase SQC (analogous to mechanism m-1). This can be done by using a flip angle filter on the read pulse of the DQF since each term has a different dependency on this angle. The dominant component (m-1) of DQC observed for taurine has a sine dependency on the angle of the read pulse,

$$1/2(2I_{Ax}I_{Xy} + 2I_{Ay}I_{Xx}) \xrightarrow{\theta_x^\circ} 1/2(2I_{Ax}I_{Xz} + 2I_{Az}I_{Xx})\sin\theta, \quad [7]$$

whereas the dominant (m-2) process for myo-inositol has a sine-cubed dependency,

$$1/2(2I_{Mx}I_{Mx} - 2I_{My}I_{My})2I_{Az} \xrightarrow{\theta_x^\circ} 4I_{Mz}I_{Mz}I_{Ay}1/2\ \sin^3\theta, \quad [8]$$

where only observable terms are given. By using a read pulse flip angle of 45° instead of 90°, it is possible to supress the m-2 mechanism by a factor of 2 relative to the m-1 mechanism, further suppressing the [5]CH myo-inositol signal. If a 22.5° read-pulse flip angle is used, the suppression factor increases to over a factor of 6. Reducing the read pulse from 90° to 45° and 22.5° reduces the intensity of taurine to 71% and 28%, respectively. Slight deviations would be expected due to the tight couplings in both taurine and myo-inositol.

In vivo resonances arising from choline and ethanolamine may still overlap with those of taurine, necessitating further editing if taurine is to be measured unequivocally. These multiplets only have couplings to resonances with chemical shifts distant from those of taurine. This difference in chemical shift can be exploited to eliminate these multiplets from the region of the spectrum occupied by taurine. If the first two 90° pulses are made semiselective (Fig. 2b), only DQCs between pairs of spins, *both* of which are perturbed by the selective pulses, will be excited. By positioning the semiselective pulse between the taurine multiplets and using sufficiently long pulse lengths, only pairs of coupled taurine and myo-inositol multiplets will be perturbed and so appear in the final spectrum. In choosing the length of the selective pulses, a number of considerations must be balanced. The effective scalar coupling evolution time can be taken from the center of the soft pulses if Gaussian waveforms are being used. Consequently, although using a long selective pulse may improve the selectivity, too long a pulse may result in the optimum scalar coupling evolution time being exceeded. Too short a selective pulse will result in unwanted multiplets being perturbed and so appearing in the final spectrum. Because the two selective pulses are symmetrically disposed about the 180° refocusing pulse, chemical shift evolution and magnetic field inhomogeneity during the pulses will be refocused during the preparation period.

In the evolution period, during the second half of the second semiselective pulse, loss of signal may occur due to chemical shift and scalar coupling evolution and dephasing due to magnetic field inhomogeneity. By introducing a hard 180° pulse followed by a delay into the evolution period (Fig. 2c) and setting the delay equal to half the semiselective pulse length, the effect of chemical shift and magnetic field inhomogeneities can be refocused.

By using a combination of the selective preparation period and the read pulse flip angle filter in the DQF, it should be possible to remove all resonances except those of taurine from the *in vivo* ^{1}H spectrum.

EXPERIMENTAL

Solutions

Individual solutions of taurine and myo-inositol were made in deuterated phosphate buffer solution at physiological pH to a concentration of approximately 0.01 M.

PCA Extracts and Brain Homogenates

PCA extracts and brain homogenates were obtained from 6-week-old female Fischer F344 rats. The animals were killed using a sodium hexabarbitone (185 mg/kg ip) overdose, and the brains were removed rapidly and freeze-clamped. Samples for PCA extraction were homogenized in perchloric acid (10/1 v/w 12% at 4°C) and the solid removed by centrifugation (3000 rpm for 30 min at 4°C). Neutralization was performed using a mixture of KOH (1.5 M), KCl (0.3 M), and Na_3PO_4 (0.1 M), and the pH was adjusted to 7.35 ± 0.05. Precipitated salt was removed by centrifugation (3000 rpm for 5 min) and the resulting clear solutions were freeze-dried to constant weight to yield white powders. The samples were reconstituted in 0.5 ml D_2O for NMR analysis.

Brain homogenates were prepared by manual homogenization in 0.5 ml D_2O to enable a lock signal. The resulting goo was then transferred into an NMR tube for analysis.

NMR Spectroscopy Studies

All spectra were acquired on a Bruker ARX 250 NMR spectrometer operating at 250 MHz for ^{1}H. *In vitro* and *in situ* spectra were referenced for chemical shift using the NAA

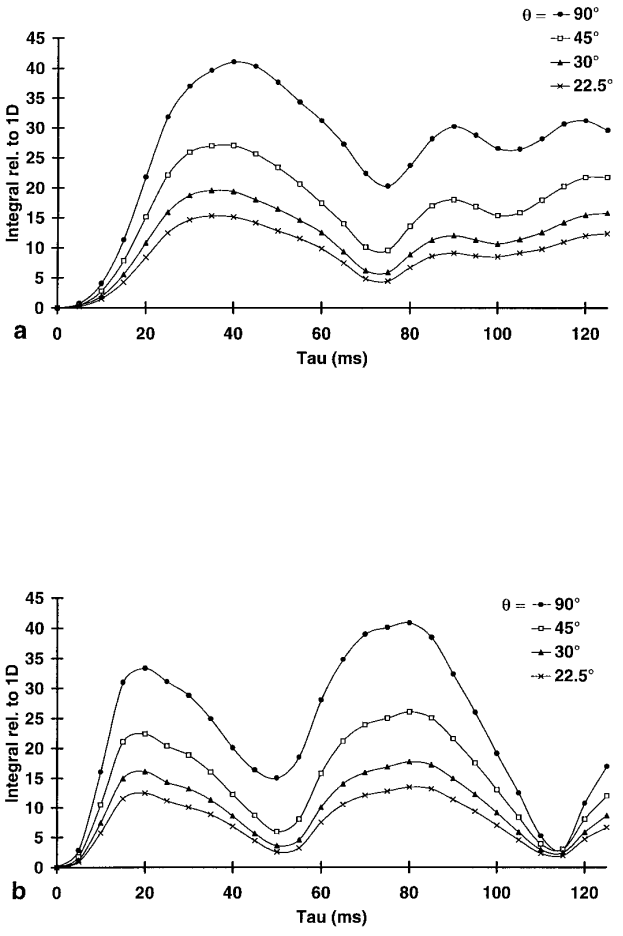

FIG. 3. Graph of the relationship between peak integral and the length of the preparation period τ using the pulse sequence given in Fig. 2a for (a) taurine and (b) myo-inositol [5]CH. Data are presented for different values of θ as given on the figure.

methyl singlet, with the resonance taken as 2.02 ppm. All experiments were carried out at 298 K.

For the data given in Fig. 1b–d, the pulse sequence given in Fig. 2a was used on a PCA rat brain extract using a τ value of 50 ms, a τ' value of 40 ms with $t_1 = 3$ μs and read pulse angles (θ) of (b) 90°, (c) 45°, and (d) 22.5°. Figure 1e–g spectra were obtained using the pulse sequence given in Fig. 2b using 20-ms Gaussian pulses placed in-between the two taurine multiplets (at 3.35 ppm) with $\tau = 44$ ms, $\tau' = 40$ ms, $t_1 = 3$ μs with read pulse angles (θ) of (e) 90°, (f) 45°, and (g) 22.5°. All spectra (a–e) were acquired with 1024 transients and are shown to the same vertical scale.

The data given in Figs. 3 and 4 was acquired with the pulse sequence given in Fig. 2a without the detection period (τ') using solutions of taurine and myo-inositol. For the data given in Fig. 3 the pulse θ and τ was varied as indicated in the figure with $t_1 = 3$ μs. The magnitude spectrum was calculated and baseline corrected before integration of the whole multiplet (for taurine the SCH_2 multiplet at 3.43 ppm and for myo-inositol the [5]CH at 3.28 ppm). For the data given in Fig. 4, τ was varied as indicated in the figure with $t_1 = 3$ μs and the read pulse (θ) equal to 90°, and the data was weighted with a sine-squared function before Fourier transformation. The magnitude spectrum was calculated and baseline corrected before integration of each transition (multiplets as given for Fig. 3).

For the data given in Fig. 5 the pulse sequence given in Fig. 2b was used on solutions of taurine and myo-inositol. The angles of all pulses were misset as indicated in the figure with $\tau = 44$ ms, $\tau' = 40$ ms, $t_1 = 3$ μs and the read pulse angles (θ) equal to 90°. The data presented is the sum of all the transition intensities of the multiplets.

Figure 6a shows a conventional 1D spectrum of rat brain homogenate. The spectra given in Fig. 6b and c were obtained using the pulse sequence given in Fig. 2b with 20-ms Gaussian pulses placed in between the two taurine multiplets (at ~3.3 ppm) with $\tau = 44$ ms, $\tau' = 40$ ms, $t_1 = 3$ μs with read pulse angles (θ) of (b) 45° and (c) 22.5°. Line broadening of 6 Hz was applied to the data. All spectra (a–c) were acquired with 512 transients and are to the same scale except for (a), which is reduced by a factor of 15.

RESULTS AND DISCUSSION

The effect of the preparation period length of the DQF given in Fig. 2a using a 90° read pulse on the integrated signal intensity for both taurine and the myo-inositol [5]CH proton can be seen in Figs. 3a and b respectively (solid circles). The myo-inositol [5]CH magnetization shows the features predicted by the product operator calculations. At $\tau = 115$ ms the intensity of the myo-inositol magnetization passes through a minimum. This corresponds to the scalar coupling evolution time of $1/J$ where both mechanisms m-1 and m-2 pass through zero. The ''dip'' predicted at $1/2J$, where no magnetization passes through the m-1 mechanism, can be clearly seen at 50 ms. The myo-inositol dip is lower than predicted by the product operator calculations, and this is attributed to the tight coupling of the [1,6]CHs to the [2,4]CHs. More importantly, this value is relatively close to the optimum τ value for taurine at 40 ms.

The corresponding graphs for the individual transitions of the taurine and myo-inositol [5]CH multiplets are given in Fig. 4. The contribution of the magnetization passing through antiphase DQC via the m-2 mechanism can be discerned from the central transitions. In theory the inner transition for both taurine and the myo-inositol [5]CH arises solely through this mechanism, whereas the outer transitions arise from a combination of both mechanisms. Deviations from the predicted behavior (Eq. [6]) probably arise from tight coupling. It can be clearly seen that the signal for myo-inositol [5]CH at the ''dip'' at 50 ms arises largely from the m-2 mechanism. The contribution of this mechanism to the taurine signal intensity at this τ value is much smaller than that for the [5]CH of myo-inositol with the intensity of the central transition being lower than the

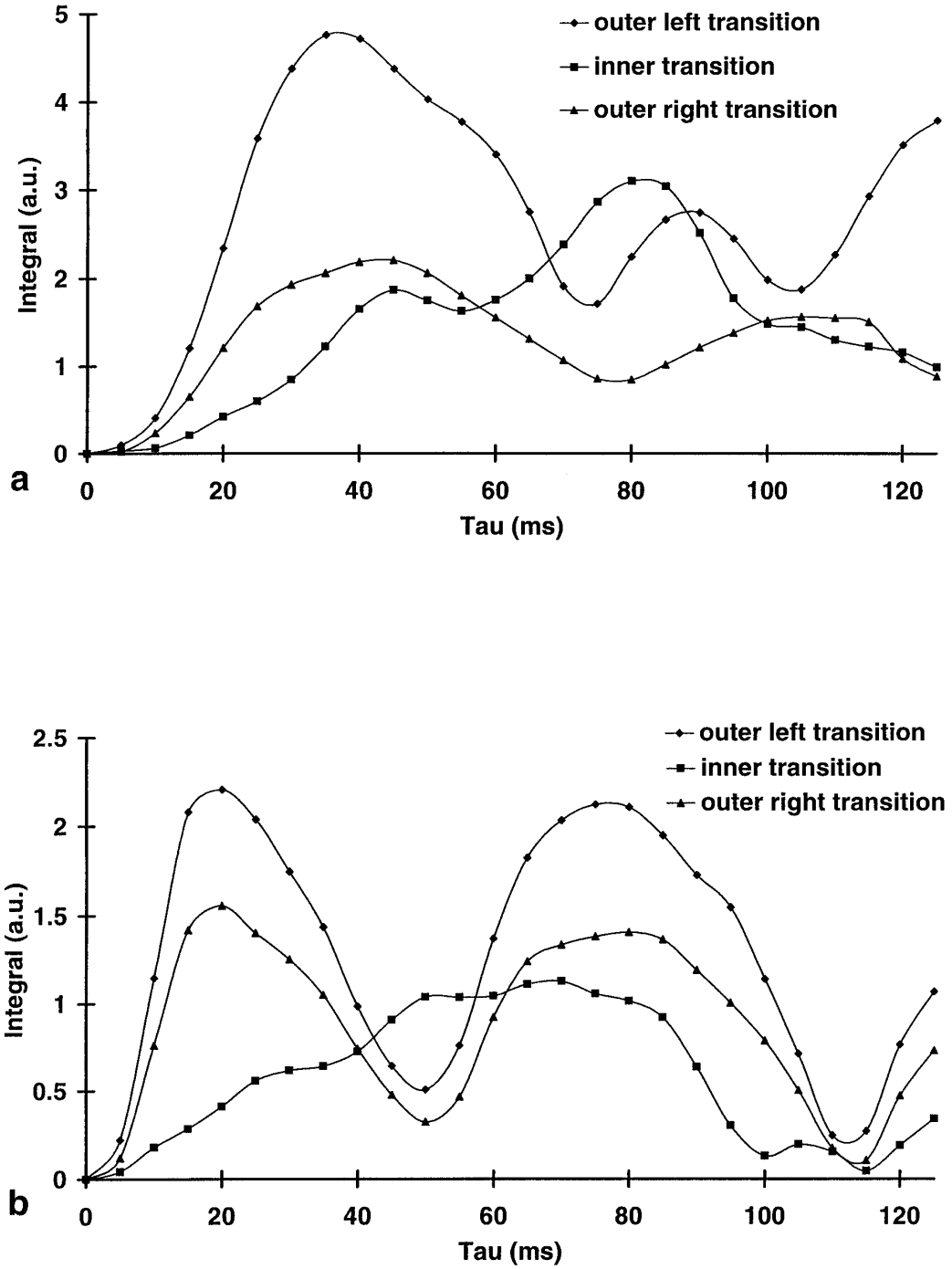

FIG. 4. Graph of the relationship between individual transition integrals and the length for the preparation period τ using the pulse sequence given in Fig. 2a for (a) taurine and (b) myo-inositol [5]CH.

outer transitions. The relatively large deviations of taurine from its predicted behavior probably arise because it is an AA′XX′ spin system, although it has been approximated to an A_2X_2 spin system for ease of calculation.

The effect of the DQF given in Fig. 2a on rat brain perchloric acid extract metabolite solution can be seen in Fig. 1b ($\theta = 90°$), with τ corresponding to the myo-inositol ''dip'' at 50 ms. The filter has successfully removed the singlets from the spectrum. As the 3.47-ppm taurine multiplet is free from other overlapping metabolites, the two taurine multiplets should appear similar if the filter has successfully removed the myo-inositol [5]CH multiplet. Comparison of the two taurine multiplets reveals that the 3.27-ppm multiplet overlaps with residual signal arising from the [5]CH of myo-inositol. The

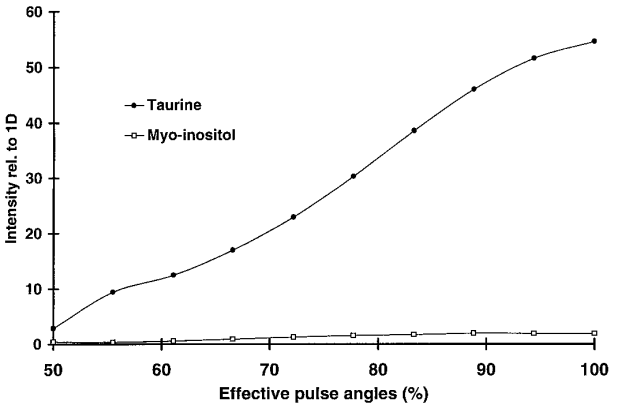

FIG. 5. Graph of the relationship between the effective pulse angle and the signal intensity of the taurine and myo-inositol [5]CH multiplets relative to a conventional 1D spectrum using the pulse sequence given in Fig. 2c.

myo-inositol signal is due to magnetization which has followed the m-2 pathway. Since the taurine signal is filtered through via the m-1 mechanism, the magnetization of the [5]CH myo-inositol can be further suppressed using the flip angle filter described by Eqs. [7] and [8]. The effect of reducing the angle of the read pulse on the overall signal intensity can be seen in Fig. 3. This shows that using a read pulse flip angle of 45° instead of 90° reduces the myo-inositol [5]CH signal intensity to 39%, whereas the taurine signal intensity is only reduced to 62%, giving an increased suppression factor of 1.6. Similarly, if the read pulse angle is reduced from 90° to 22.5° the myo-inositol signal intensity is reduced to 17% while that of taurine is reduced to 34%, giving an increased suppression factor of 2.0. The suppression is less than that predicted by the product operator calculations (Eqs. [7] and [8]). This can be attributed to the fact that some of the taurine magnetization passes through the m-2 mechanism (Fig. 4) and to tight coupling. The results of using the pulse sequence given in Fig. 2a with various read pulse flip angles can be seen in Fig. 1b–d. By reducing the read pulse flip angle to 22.5° the myo-inositol signal has been diminished to a negligible amount.

Although the filter has successfully removed the singlets from the spectrum, the taurine multiplets will still overlap with choline and ethanolamine (depending on ischemic state) *in vivo.* Therefore, there is a need for further selectivity if the taurine is to be observed unequivocally. By using the selective preparation period as shown in Fig. 2b, it is possible to remove these unwanted resonances. Gaussian selective pulses (*37*) were used. Their optimum length at 250 MHz was found to be 20 ms. Optimization of the sequence revealed little change from the sequence given in Fig. 2a with the intensity of the myo-inositol multiplet passing through a dip at a τ value of 44 ms, where the corresponding taurine intensity is still approximately 80% of its maximum.

The DQF given in Fig. 2b was demonstrated on a rat brain perchloric acid extract with the 20-ms Gaussian pulses placed halfway between the two taurine multiplets in Fig. 1e. The taurine multiplets are well resolved with very little evidence of myo-inositol. It is important to note that the taurine resonances are in-phase; this means that signal will not be lost as a result of the broadening of spectral lines encountered *in vivo.* Compared to conventional 1D spectra obtained under similar conditions, the efficiency is 35% for taurine and 2.5% for myo-inositol, taking all of the transitions of a multiplet into account. Figures 1e–1g shows the effect of the read pulse flip angle filter on the selective preparation period experiment as shown in Fig. 2b. Since the filter containing the selective preparation periods is quite efficient at removing the undesirable myo-inositol [5]CH, the read pulse flip angle filter gave no appreciable increase in the myo-inositol suppression at smaller angles. This is because the [4,6]CHs of myo-inositol are less efficiently excited by the soft pulses. To overcome any signal loss due to chemical shift evolution and dephasing due to magnetic field inhomogeneity during the second half of the second selective

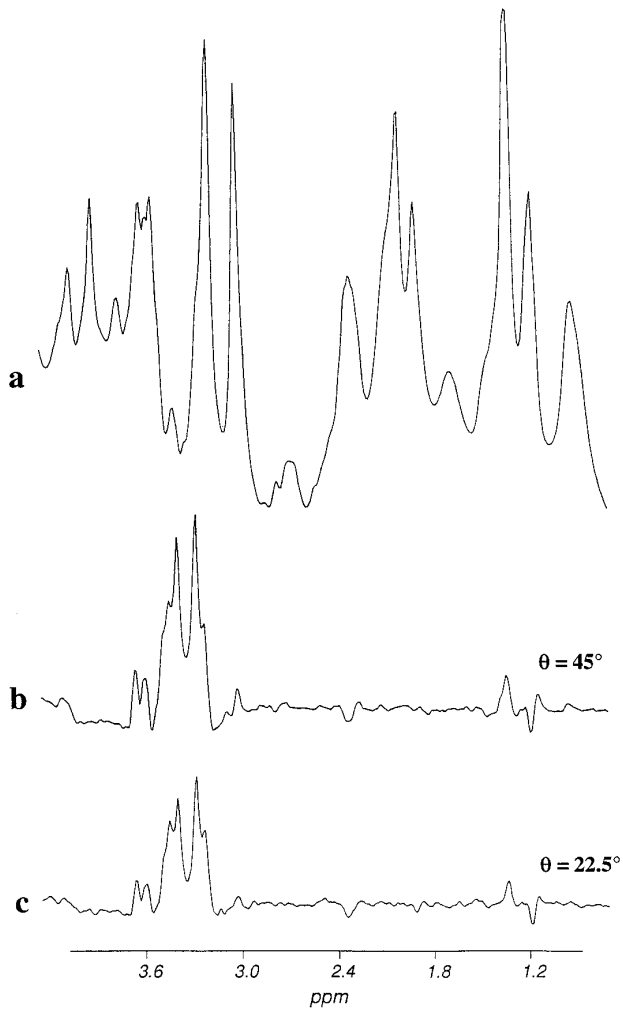

FIG. 6. 250-MHz *in situ* proton spectra of a homogenized rat brain. (a) Conventional 1D. (b, c) Spectrum obtained using the same parameters as in Fig. 1 (f, g) respectively. The spectra are displayed with (b, c) scaled up by a factor of 15 relative to (a).

pulse, the sequence given in Fig. 2c was also tried. This sequence contains a 180° pulse to refocus these effects. However, this pulse sequence gave no significant improvement.

To assess the technique's usefulness, the efficiency with which it passes taurine and the size of the residual signal arising from overlapping metabolites were determined at 250, 200, and 150 MHz. This was achieved using experimental data at 250 MHz and simulated data at the other frequencies. Simulations were calculated using the full density matrix and the same parameters as used in the experiments with the aid of the GAMMA NMR simulation library (*38*). *In vivo* taurine is typically found at concentrations of 1.2–1.5 mmol kg^{-1}, whereas myo-inositol is typically found at concentrations of 4.7–6.8 mmol kg^{-1} (*39*). However, although myo-inositol only contributes one proton to the region of interest of the spectrum, taurine contributes two if one multiplet is being measured or four if both are, which may be more practicable *in vivo;* the taurine multiplet at 3.27 ppm overlaps with that of myo-inositol, while that at 3.43 ppm does not. The efficiency with which taurine passes through the filter is 35% at 250 MHz, 30% at 200 MHz, and 15% at 150 MHz, assuming that the read pulse angle is 90°. The error introduced into the measurement as a result of residual myo-inositol magnetization, assuming that both taurine multiplets are measured, will be 5.5–10% at 250 MHz, 7.7–14% at 200 MHz, and 10–19% at 150 MHz, assuming that the read pulse angle is 90°; these figures can be halved by using an angle of 22.5°. Glucose, which typically occurs at 0.8 mmol L^{-1} *in vivo* (*38*), also has resonances which overlap with those of taurine; however, it only passes through the filter with an efficiency of $<1\%$. The preceding figures have been determined from the integrals of the phased spectra. This effectively eliminates any contribution from antiphase magnetization which can be expected to cancel out *in vivo* as a result of line broadening. The reduced efficiency with which taurine is passed by the filter at lower magnetic field strengths and the increasing errors likely from overlapping metabolites means that the technique is unlikely to be useful below 150 MHz.

In order for the sequence to be of use *in vivo,* it must be robust enough to cope with misset pulses, especially if it is to be implemented with surface coils; if the pulse angles vary significantly it is possible that myo-inositol may be able to pass through the filter via another coherence transfer pathway, thus reducing the editing efficiency of the sequence. The effect on signal intensity of varying the effective angles of all pulses in unison for the pulse sequence given in Fig. 2b can be seen in Fig. 5. As the taurine signal intensity decreases, so does that of the myo-inositol, thus showing that pulse angle variations do not cause the ratio of taurine to myo-inositol signal to change significantly.

Using the sequence given in Fig. 2b the experiment was tried *in situ* on a homogenized rat brain. Figure 6a shows a conventional 1D experiment while Fig. 6b shows the taurine edited spectrum. It can be seen that the signal intensity of the edited spectrum has decreased in comparison to the 1D, which can be attributed to the efficiency of the filter and relaxation effects. Figures 6b and 6c shows the effects of the read-pulse flip angle filter. Since it appeared that the myo-inositol had been suppressed by the filter it is difficult to tell if the flip angle had any significant effect. Clearly, unlike with the PCA brain extract, the 3.43-ppm taurine multiplet has some residual signal overlapping, and consequently, it is difficult to assess the effectiveness of editing by comparing the two taurine multiplets.

CONCLUSION

By combining four spectral editing procedures we have produced a new pulse sequence which allows observation of both taurine multiplets *in vitro* and *in situ* free from overlapping metabolite resonances. By using a DQF, scalar coupling evolution time, chemical shift selectivity (with soft pulses), and a read-pulse flip angle filter, we have removed the surrounding metabolite resonances, giving a clean spectrum of taurine. The technique is robust enough to be implemented with a surface coil. Work is currently underway to apply this sequence *in vivo.*

ACKNOWLEDGMENTS

We thank the Centre for Mechanisms of Human Toxicity (University of Leicester) for use of the 250-MHz spectrometer and Dr. S. C. R. Williams (Department of Neurology, Institute of Psychiatry) for helpful discussions.

REFERENCES

1. C. E. Wright, H. H. Tallan, Y. Y. Lin, and G. E. Gaull, *Ann. Rev. Biochem.* **55,** 427 (1986).
2. R. W. Chesney, *Adv. Pediatr.* **32,** 1 (1985).
3. R. J. Huxtable, *Prog. Neurobiol.* **32,** 471 (1989).
4. R. J. Huxtable, *Physiol. Rev.* **72,** 101 (1992).
5. W. Walz and A. F. Allen, *Exp. Brain Res.* **68,** 290 (1987).
6. J. G. Verbalis and S. R. Gullans, *Brain Res.* **567,** 274 (1991).
7. W. Stummer, A. L. Betz, P. Shakui, and R. F. Keep, *J. Cereb. Blood Flow Metab.* **15,** 8 (1995).
8. J. A. Sturman, D. K. Rassin, and G. E. Gaull, *J. Neurochem.* **28,** 31 (1977).
9. K. Hida, I. L. Kwee, and T. Nakada, *Magn. Reson. Med.* **23,** 31 (1992).
10. T. E. Bates, S. R. Williams, D. G. Gadian, J. D. Bell, R. K. Small, and R. A. Iles, *NMR Biomed.* **2,** 225 (1989).
11. R. Barri, P. Bigler, P. Straehl, S. Posse, J.-P. Colombo, and N. Herschkowitz, *Neurochem. Res.* **15,** 1009 (1990).
12. T. Michaelis, K.-D. Merboldt, W. Hänicke, M. L. Gyngell, H. Bruhn, and J. Frahm, *NMR Biomed.* **4,** 90 (1991).
13. D. L. Rothman, K. L. Behar, H. P. Hetherington, and R. G. Shulman, *Proc. Natl. Acad. Sci. USA* **81,** 6330 (1984).
14. C. Bauer and R. Freeman, *J. Magn. Reson.* **61,** 376 (1985).
15. R. Freeman and S. Wittekoek, *J. Magn. Reson.* **1,** 238 (1969).

16. H. P. Hetherington, M. J. Avison, and R. G. Shulman, *Proc. Natl. Acad. Sci. USA* **82,** 3115 (1985).
17. L. D. Hall and T. J. Norwood, *J. Magn. Reson.* **78,** 582 (1988).
18. D. L. Rothman, O. A. C. Petroff, K. L. Behar, and R. H. Mattson, *Proc. Natl. Acad. Sci. USA* **90,** 5662 (1993).
19. T. J. Norwood, *Prog. NMR Spectrosc.* **24,** 295 (1992).
20. A. Bax, R. Freeman, and S. P. Kempsell, *J. Am. Chem. Soc.* **102,** 4849 (1980).
21. O. W. Sørensen, M. H. Levitt, and R. R. Ernst, *J. Magn. Reson.* **55,** 104 (1983).
22. M. Rance, O. W. Sørensen, W. Leupin, H. Kogler, K. Wuthrich, and R. R. Ernst, *J. Magn. Reson.* **61,** 67 (1985).
23. O. W. Sørensen, M. Rance, and R. R. Ernst, *J. Magn. Reson.* **56,** 527 (1984).
24. U. Piantini, O. W. Sørensen, and R. R. Ernst, *J. Am. Chem. Soc.* **104,** 6800 (1982).
25. A. J. Shaka and R. Freeman, *J. Magn. Reson.* **51,** 169 (1983).
26. M. Rance, O. W. Sørensen, G. Bodenhausen, G. Wagner, R. R. Ernst, and K. Wüthrich, *Biochem. Biophys. Res. Commun.* **117,** 479 (1983).
27. J. E. van Dijk, A. F. Mehlkopf, and W. M. M. J. Bovee, *NMR Biomed.* **5,** 75 (1992).
28. C. H. Sotak, D. M. Freeman, and R. E. Hurd, *J. Magn. Reson.* **23,** 355 (1988).
29. R. E. Hurd and D. M. Freeman, *Proc. Natl. Acad. Sci. USA* **86,** 4402 (1989).
30. A. Knüttel and R. Kimmich, *Magn. Reson. Med.* **10,** 404 (1989).
31. L. A. Trimble, J. F. Shen, A. H. Wilman, and P. S. Allen, *J. Magn. Reson.* **86,** 191 (1990).
32. W.-I. Jung and O. Lutz, *J. Magn. Reson.* **94,** 587 (1991).
33. A. H. Wilman and P. S. Allen, *J. Magn. Reson. B* **101,** 165 (1993).
34. D. L. Hardy, R. W. Wilson, T. Jessel, S. C. R. Williams, S. C. Smart, and T. J. Norwood, *J. Magn. Reson. B* **111,** 97 (1996).
35. D. Freeman and R. Hurd, *NMR Basic Princ. Prog.* **27,** 199 (1992).
36. O. W. Sørensen, G. W. Eich, M. H. Levitt, G. Bodenhausen, and R. R. Ernst, *Progr. NMR Spectrosc.* **16,** 163 (1983).
37. C. Bauer, R. Freeman, T. Frenkiel, J. Keeler, and A. J. Shaka, *J. Magn. Reson.* **58,** 442 (1984).
38. S. A. Smith, T. O. Levante, B. H. Meier, and R. R. Ernst, *J. Magn. Reson. A* **106,** 75 (1994).
39. T. Michaelis, K.-D. Merboldt, H. Bruhn, W. Hänicke, and J. Frahm, *Radiology* **187,** 219 (1993).